

Synthesis and Characterization of New Diazenecarboxamide Ligands Using a Selective Adduct Formation with $B(C_6F_5)_3$

Manuel A. Escobar,^a Mauricio Valderrama,^a Constantin G. Daniliuc^b and Rene S. Rojas^{*a}

^aDepartamento de Química Inorgánica, Facultad de Química, Pontificia Universidad Católica de Chile, Casilla 306, Santiago-22, Chile

^bOrganisch-Chemisches Institut, Universität Münster, Corrensstrasse 40, 48149, Münster, Germany

The synthesis and structure of new *N*-(2,6-diisopropylphenyl)-2-phenyldiazenecarboxamide (L_2) and *N*-(2,6-diisopropylphenyl)-2-(perfluorophenyl) diazenecarboxamide (L_3) ligands are described. The subsequent reactions of ligands L_1 , L_2 and L_3 with tris(pentafluorophenyl)borane gave rise to new adducts (A_1), (A_2) and (A_3), where $B(C_6F_5)_3$ is coordinated to the carbonyl group. New ligands and adducts are characterized by nuclear magnetic resonance (NMR), infrared (IR), and elemental analysis techniques. The crystal structures of all compounds are obtained and described.

Keywords: diazenecarboxamide ligands, borane adduct, azo compounds

Introduction

Azo compounds have caused great interest in organic synthesis,^{1,2} they have been utilized as dyes and analytical reagents,³ and as a material for non linear optics and for optics information storage in laser disks.^{4,5} Recently, many studies have shown that some azo compounds possess excellent optical memory and photoelectric properties.^{6,7}

These types of ligands have been explored also as potential modulators of drug resistance to cisplatin for certain types of tumors,^{8,9} but their coordination chemistry has not been explored.

Among the variety of organic compounds that can act as ligands, the diazenecarboximides seem to be good candidates because of their structural “similarity” with α -iminocarboxamides, especially considering the various modes of coordination that they can present (NN, NO and η^3 -NO).

The basis of the development of new catalysts for different processes continues to be centered on the design of organic compounds capable not only to stabilize a metallic center, but also to allow greater control of their reactivity and selectivity in a given catalytic process.¹⁰⁻¹⁸ An interesting series of catalysts similar to α -diimines¹⁹⁻²² have been reported recently (Figure 2),²³⁻²⁹ in which the ligands contain Lewis base groups such as cyano, carbonyl or other heteroatoms in addition to those coordinated with the metallic center, i.e., with exocyclic functionalities.

We have therefore focused on the design of a series of new diazenecarboxamide ligands differing in electronic and steric properties. We have prepared the corresponding adduct with $B(C_6F_5)_3$ (BCF) to deduce how it interacts with the heteroatoms in the molecule and if the ligand has a preferred site of coordination to a Lewis acid.

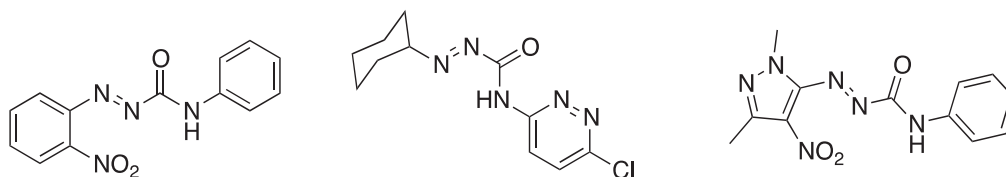


Figure 1. Azo compounds.

*e-mail: rrojasg@uc.cl

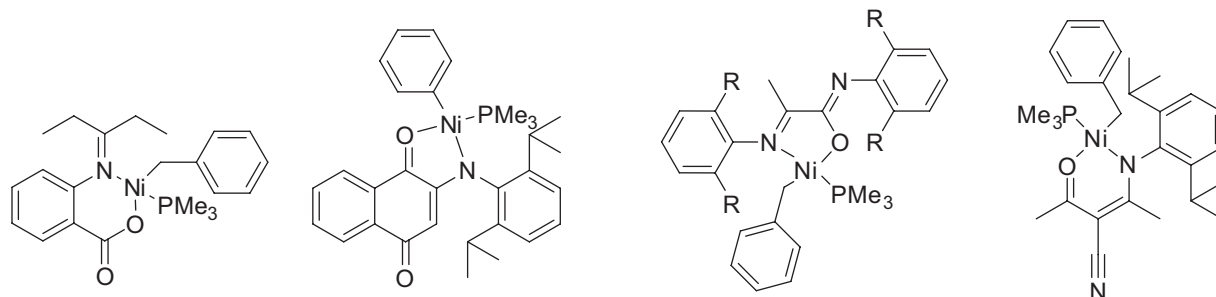


Figure 2. Examples of complexes with basic exocyclic functionalities.

Experimental

All manipulations were performed under an inert atmosphere using standard glovebox and Schlenk-line techniques. All reagents were used as received from Aldrich, unless otherwise specified. Toluene, tetrahydrofuran (THF), ether, and pentane were distilled from benzophenone ketyl. Tris(pentafluorophenyl)borane ($\text{B}(\text{C}_6\text{F}_5)_3$) was sublimed at 65 °C under static vacuum and stored in the glovebox. The following instruments were used for the physical characterization of the compounds. Nuclear magnetic resonance (NMR) spectra were obtained on Bruker DRX 400, AVANCE 400 MHz, and AVANCE III 400 MHz spectrometers. ^1H and ^{13}C $\{^1\text{H}\}$ chemical shifts were referenced to residual proton and naturally abundant ^{13}C resonances of the deuterated solvent, respectively, relative to tetramethylsilane. Most NMR assignments were supported by additional 2D experiments. Infrared (IR) spectra were recorded on a Bruker Vector-22 spectrophotometer using KBr pellets, and in solution using C_6D_6 as solvent.

Synthesis of *N*,2-diphenyldiazene-carboxamide (L_1)

Phenyl isocyanate (1.38 g; 11.6 mmol) was added to a solution of phenylhydrazine (1.25 g; 11.6 mmol) in anhydrous acetonitrile (40 mL). The mixture was stirred for 1 h. A white precipitate was formed. The solvent was evaporated under vacuum to obtain (2.39 g; 10.5 mmol) of intermediate product $\text{C}_6\text{H}_5\text{NHNHCONHC}_6\text{H}_5$. The crude product was then suspended in a mixture of $\text{CH}_2\text{Cl}_2/\text{CH}_3\text{CH}_2\text{OH}$ (5:1) and pyridine (0.83 g; 10.5 mmol). The solution was cooled in water, and (1.91 g; 10.7 mmol) *N*-bromosuccinimide was added dropwise during 5 min with stirring. The solution changed its color to deep red. The resulting solution was stirred for 10 min at room temperature and was washed consecutively with water (2×15 mL), 10% NaOH (10 mL), and water (2×15 mL). The solution was dried over MgSO_4 , filtered and evaporated under vacuum. The crude product was dissolved in

minimum amounts of methanol and recrystallized; an orange solid was obtained and washed with cool hexane, yield 2.07 g (79.5%).

IR (KBr) ν_{max} / cm^{-1} 3261, 3233, 3192, 3134, 3078, 3060, 3020, 1700, 1604, 1555, 1492, 1442, 1319, 1306, 1254, 1180, 1142, 976, 779, 756, 692, 681, 574, 498, 472; ^1H NMR (400 MHz, CD_2Cl_2) δ 8.69 (s, 1H, NH), 7.96 (d, 2H, J 7.1 Hz, Ar-H), 7.75 (d, 2H, J 7.5 Hz, Ar-H), 7.62 (t, 1H, Ar-H), 7.55 (t, 2H, J 7.4 Hz, Ar-H), 7.42 (t, 2H, Ar-H), 7.21 (t, 1H, J 7.4 Hz, Ar-H); ^{13}C NMR (100 MHz, CD_2Cl_2) δ 157.9, 151.6, 137.6, 134.6, 130.0, 129.8, 125.6, 124.5, 120.3; anal. calcd. for $\text{C}_{13}\text{H}_{11}\text{N}_3\text{O}$: C, 69.32; H, 4.92; N, 18.66; found: C, 69.27; H, 4.56; N, 18.81.

N-(2,6-Diisopropylphenyl)-2-phenyldiazene-carboxamide (L_2)

Using the same procedure as for the synthesis of L_1 , (2,6-diisopropylphenyl)isocyanate (0.79 g; 3.91 mmol), phenylhydrazine (0.42 g; 3.91 mmol), $\text{C}_6\text{H}_5\text{NHNHCONH}$ 2,6-*iPr* $_2\text{C}_6\text{H}_3$ (0.84 g; 2.71 mmol), pyridine (0.21 g; 2.71 mmol) and *N*-bromosuccinimide (0.49 g; 2.75 mmol) were used to obtain the orange solid L_2 ; yield 0.63 g (52%).

IR (KBr) ν_{max} / cm^{-1} 3231, 3056, 2965, 1702, 1498, 1468, 1451, 1217, 1203, 1183, 1153, 796, 781, 762, 730, 684; ^1H NMR (400 MHz, CD_2Cl_2) δ 8.03 (d, 2H, J 7.0 Hz, Ar-H), 7.88 (s, 1H, NH), 7.65 (m, 1H, Ar-H), 7.61 (m, 2H, Ar-H), 7.40 (t, 1H, J 7.7 Hz, Ar-H), 7.28 (d, 2H, J 7.8 Hz, Ar-H), 3.19 (m, 2H, J 6.9 Hz, CH-*iPr*), 1.23 (d, 6H, J 6.9 Hz, CH_3); ^{13}C NMR (100 MHz, CD_2Cl_2) δ 160.4, 151.7, 147.2, 134.5, 130.8, 130.0, 129.4, 124.6, 124.3, 29.4, 24.0; anal. calcd. for $\text{C}_{19}\text{H}_{23}\text{N}_3\text{O}$: C, 73.76; H, 7.49; N, 13.58; found: C, 73.47; H, 7.51; N, 13.68.

N-(2,6-Diisopropylphenyl)-2-(perfluorophenyl)diazene-carboxamide (L_3)

Using the same procedure as for the synthesis of L_1 , (2,6-diisopropylphenyl)isocyanate (1.50 g; 7.4 mmol), pentafluorophenyl hydrazine (1.4 g; 7.4 mmol), $\text{C}_6\text{F}_5\text{NHNHCONH}$ 2,6-*iPr* $_2\text{C}_6\text{H}_3$ (2.7 g; 6.7 mmol),

pyridine (0.53 g; 6.7 mmol) and *N*-bromosuccinimide (1.24 g; 6.9 mmol) were used to obtain the orange solid L₃; yield 1.43 g (49%).

IR (KBr) ν_{\max} / cm^{-1} 3187, 2969, 1693, 1523, 1515, 1491, 1407, 1313, 1135, 1032, 975, 798, 748; ¹H NMR (400 MHz, CD₂Cl₂) δ 7.80 (s, 1H, NH), 7.41 (t, 1H, *J* 7.7 Hz, Ar-H), 7.28 (d, 2H, *J* 7.7 Hz, Ar-H), 3.16 (m, 2H, *J* 6.8 Hz, CH-*i*Pr), 1.24 (d, 6H, *J* 6.8 Hz, CH₃-*i*Pr); ¹³C NMR (100 MHz, CD₂Cl₂) δ 159.3, 147.0, 130.1, 129.8, 124.4, 29.5, 24.0; anal. calcd. for C₁₉H₁₈F₅N₃O: C, 57.14; H, 4.54; N, 10.52; found: C, 57.25; H, 4.08; N, 10.64.

N,2-Diphenyldiazenecarboxamide-B(C₆F₅)₃ (A₁)

A solution of B(C₆F₅)₃ (0.11 g; 0.13 mmol) in anhydrous dichloromethane was added to L₁ (0.05 g; 0.13 mmol) previously dissolved in anhydrous dichloromethane. The mixture was stirred for 2 h at RT. The solution was filtered and evaporated to dryness. The solid was washed twice with anhydrous pentane and dried in vacuum to obtain A₁ as a red solid in quantitative yield. Single red crystals of A₁ suitable for X-ray crystal structure analysis were obtained from dichloromethane/pentane by the diffusion method.

IR (KBr) ν_{\max} / cm^{-1} 3337, 3067, 2978, 2958, 2936, 2874, 1649, 1585, 1518, 1454, 1381, 1353, 1316, 1247, 1207, 1152, 978, 766, 674; ¹H NMR (400 MHz, CD₂Cl₂) δ 9.22 (s, 1H, NH), 7.83 (dd, 2H, Ar-H), 7.79 (t, 1H, *J* 7.7 Hz, Ar-H), 7.69 (dd, 2H, *J* 7.7 Hz, Ar-H), 7.61 (t, 2H, *J* 7.7 Hz, Ar-H), 7.53 (t, 2H, *J* 7.7 Hz, Ar-H), 7.47 (t, 1H, *J* 7.7 Hz, Ar-H); ¹³C NMR (100 MHz, CD₂Cl₂) δ 160.8, 151.0, 138.9, 132.6, 130.9, 130.5, 129.8, 126.7, 123.2; ¹⁹F NMR (370 MHz, CD₂Cl₂) δ -132.5, -156.2, -163.4; ¹¹B NMR (160 MHz, CD₂Cl₂) -3.78 ppm ($\nu^{1/2}$ ca. 800 Hz); anal. calcd. for C₃₁H₁₁BF₁₅N₃O: C, 50.50; H, 1.50; N, 5.70; found: C, 50.30; H, 1.56; N, 5.87.

N-(2,6-Diisopropylphenyl)-2-phenyldiazenecarboxamide-B(C₆F₅)₃ adduct (A₂)

This compound was obtained by the same procedure as for the synthesis of A₁, but with B(C₆F₅)₃ (0.09 g; 0.17 mmol) and L₂ (0.05 g; 0.17 mmol).

IR (KBr) ν_{\max} / cm^{-1} 3336, 3068, 1646, 1595, 1541, 1518, 1468, 1380, 1316, 1287, 1103, 978, 782, 690, 679; ¹H NMR (400 MHz, CD₂Cl₂) δ 8.61 (s, 1H, N-H), 7.78 (m, 3H, *J* 7.7 Hz, Ar-H), 7.61 (t, 2H, *J* 7.8 Hz, Ar-H), 7.48 (t, 1H, *J* 7.8 Hz, Ar-H), 7.30 (d, 2H, *J* 7.8 Hz, Ar-H), 2.99 (m, 2H, *J* 6.7 Hz, CH-*i*Pr), 1.18 (d, 12H, *J* 6.7 Hz, CH₃); ¹³C NMR (100 MHz, CD₂Cl₂) δ 163.8, 151.3, 146.5, 138.7, 131.2, 130.8, 127.2, 126.5, 124.7, 29.2, 24.1; ¹⁹F NMR

(370 MHz, CD₂Cl₂) δ -132.5, -157.0, -164.0; ¹¹B NMR (160 MHz, CD₂Cl₂) -4.41 ppm ($\nu^{1/2}$ ca. 820 Hz); anal. calcd. for C₃₇H₂₃BF₁₅N₃O: C, 54.10; 2.82; N, 5.12; found: C, 53.80; 3.00; N, 5.23.

N-(2,6-Diisopropylphenyl)-2-(perfluorophenyl)diazenecarboxamide -B(C₆F₅)₃ adduct (A₃)

This compound was obtained by the same procedure as for the synthesis of A₁, but with B(C₆F₅)₃ (0.06 g; 0.13 mmol) and L₃ (0.05 g; 0.13 mmol).

IR (KBr) ν_{\max} / cm^{-1} 3371, 2973, 2935, 1647, 1519, 1468, 1397, 1330, 1288, 1259, 1172, 1106, 1035, 980, 801, 678; ¹H NMR (400 MHz, CD₂Cl₂) δ 8.49 (s, 1H, NH), 7.48 (t, 1H, *J* 7.8 Hz, Ar-H), 7.29 (d, 2H, *J* 7.8 Hz, Ar-H), 2.95 (m, 2H, *J* 6.8 Hz, CH-*i*Pr), 1.15 (d, 6H, *J* 6.8 Hz, CH₃); ¹³C NMR (100 MHz, CD₂Cl₂) δ 163.1, 146.4, 127.1, 131.3, 124.8, 29.4, 23.7; ¹⁹F NMR (370 MHz, CD₂Cl₂) δ -132.2, -132.9, -155.8, -156.7, -162.3, -163.1; ¹¹B NMR (160 MHz, CD₂Cl₂) -6.02 ppm ($\nu^{1/2}$ ca. 1100 Hz); anal. calcd. for C₃₇H₁₈BF₂₀N₃O: C, 48.76; H, 1.99; N, 4.61; found: C, 49.01; H, 2.15; N, 4.67.

X-ray diffraction

Data sets were collected with a Nonius KappaCCD diffractometer. Programs used: data collection, COLLECT;³⁰ data reduction Denzo-SMN;³¹ absorption correction, Denzo;³² structure solution SHELXS-97;³³ structure refinement SHELXL-97³⁴ and graphics, XP.³⁵ Thermal ellipsoids are shown with 30% probability, R-values are given for observed reflections, and wR² values are given for all reflections.

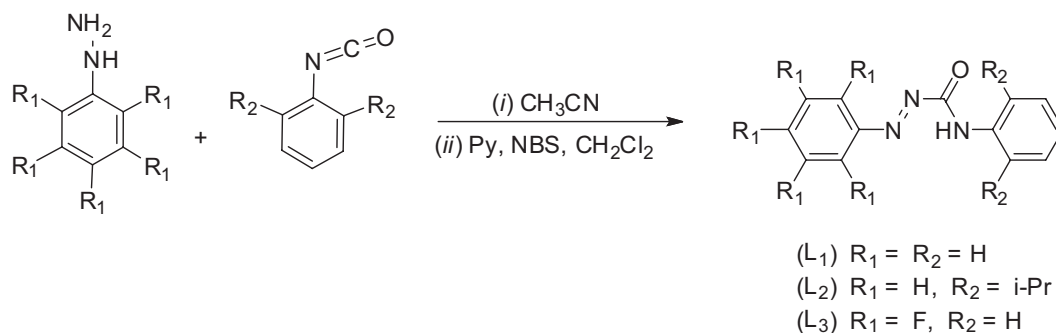
Exceptions and special features

Compounds L₁, L₃ and A₃ crystallized with two molecules in the asymmetric unit. In all compounds (L₁, L₂, L₃, A₁, A₂ and A₃) the hydrogen atom at nitrogen N1 was refined freely.

Results and Discussion

Synthesis of ligands

Scheme 1 shows the synthetic pathway to the diazenecarboxamide ligand.^{8,36} The reaction sequence begins with the addition of the monosubstituted hydrazine derivative to the isocyanate at RT, resulting in the formation of the corresponding 1,4-disubstituted semicarbazide. Oxidation of the semicarbazide with *N*-bromosuccinimide/pyridine



Scheme 1. Synthetic pathway to the diazenecarboxamide ligand.

Table 1. Selected spectroscopic parameters of the diazenecarboxamide ligands L₁, L₂, L₃, and the diazenecarboxamide-BCF adducts A₁, A₂ and A₃

	L ₁	L ₂	L ₃	A ₁	A ₂	A ₃
NMR δ ¹ H / ppm						
N–H	8.69	8.03	7.80	9.22	8.61	8.49
HC ^{<i>i</i>Pr}	–	3.19	3.16	–	2.99	2.95
Me ^{<i>i</i>Pr}	–	1.23	1.24	–	1.18	1.15
NMR δ ¹³ C / ppm						
(C=O)	157.9	160.4	159.3	160.8	163.8	162.9
FTIR / cm ⁻¹						
ν(C=O)	1700	1702	1693	1646	1649	1648

(NBS/Py) yields the desired compound. See Experimental and Supplementary Information (SI) sections.

The symmetric (L₁)³⁷ and asymmetric (L₂ and L₃) diazenecarboxamide ligands were purified by crystallization in methanol, in 80, 52 and 49% yield, respectively. In each case the ¹H, ¹³C NMR spectra (in [D₂]-dichloromethane) are consistent with the exclusive formation of one product. In the case of L₃, the three signals in the ¹⁹F NMR spectrum at –138.8(*o*), –139.3(*p*), and –153.9(*m*) ppm confirm the formation of this compound. For details, see Table 1 and SI section.

FTIR spectroscopy shows bands at 1700, 1702 and 1693 cm⁻¹ for L₁, L₂ and L₃, respectively, due to the C=O functionality.

Solid-state characterization of L₁ by single-crystal X-ray diffraction (Figure 3) is consistent with the structure in Scheme 1. Compound L₁ adopts a close coplanar geometry [N4–N3–C2–N1, dihedral angle –168.7(1)°] including the two phenyl rings with a *trans* relation around the N=N double bond between the phenyl and the carboxamide oxygen fragment (Table 2). Angles O1–C2–N1 and O1–C2–N3 are 127.3(1)° and 124.4(1)°, indicating a slight distortion from the ideal planar trigonal geometry, while the N3–N4, N3–C2 and N1–C2 bond distances are 1.246(2), 1.466(2) and 1.338(2) Å, consistent with a double and single bond character, respectively.

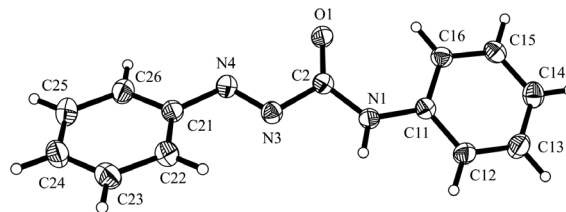


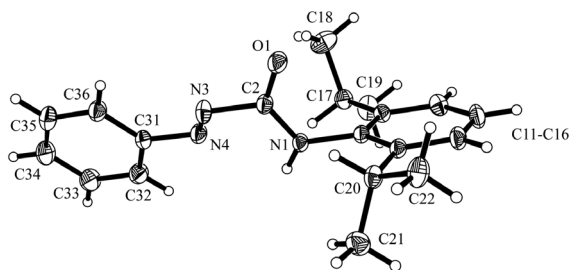
Figure 3. Molecular structure of the L₁ ligand. Only one of the two independent molecules found in the asymmetric unit is shown (thermal ellipsoids are shown at 30% probability).

Also, single crystals of L₂ suitable for X-ray diffraction studies were obtained by slow evaporation of the solvent from a concentrated ether solution at RT. The results of this study are shown in Figure 4. The molecular structure of L₂ shows that the N3–N4 bond is slightly out of the C2 sp² plane (they are not coplanar). However, N3 and N1 are on the same side of the structure. The O1–C2–N3 and O1–C2–N1 angles are not equal, [116.5(2)° and 126.8(2)°], due to increased steric hindrance near the N1 atom. The N3–N4, C2–O1 and N3–C2, N1–C2 bond distances are 1.227(3), 1.217(3) Å, and 1.464(3) and 1.333(3) Å, indicating double and single bond character, respectively. For details see Table 2 and SI section.

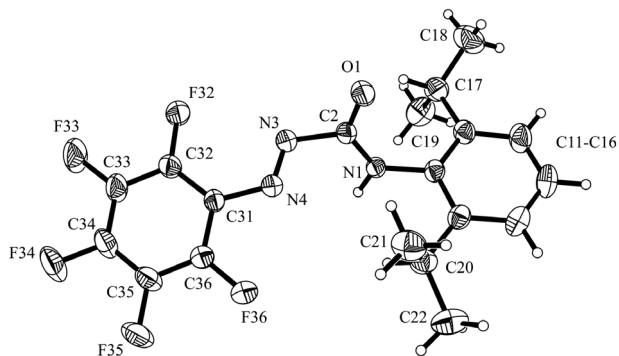
Single crystals of L₃ suited for X-ray crystal structure analysis were obtained by slow evaporation of an ether solution at RT (Figure 5). This analysis shows that ligand L₃

Table 2. Selected bond lengths (Å) and angles (degree) for compounds L₁, L₂, L₃, A₁, A₂ and A₃

	L ₁	L ₂	L ₃	A ₁	A ₂	A ₃
Bond lengths (Å)						
O(1)-C(2)	1.217(2)	1.217(3)	1.217(2)	1.260(3)	1.262(2)	1.251(4)
N(1)-C(2)	1.338(2)	1.333(3)	1.321(3)	1.308(3)	1.309(3)	1.306(5)
N(3)-C(2)	1.466(2)	1.464(3)	1.462(3)	1.423(3)	1.432(3)	1.434(5)
N(3)-N(4)	1.246(2)	1.227(3)	1.233(2)	1.249(2)	1.252(2)	1.242(4)
O(1)-B(1)	–	–	–	1.565(3)	1.577(3)	1.593(5)
Bond Angles (°)						
O(1)-C(2)-N(1)	127.3(1)	126.8(2)	128.0(2)	121.7(2)	121.1(2)	121.3(3)
O(1)-C(2)-N(3)	124.4(1)	116.5(2)	118.0(2)	118.5(2)	118.8(2)	121.8(3)
O(1)-B(1)-C(41)	–	–	–	101.1(2)	111.0(2)	109.0(3)
O(1)-B(1)-C(51)	–	–	–	108.8(2)	106.0(2)	104.5(3)
O(1)-B(1)-C(61)	–	–	–	–	102.1(2)	101.9(3)
O(1)-B(1)-C(31)	–	–	–	109.3(2)	–	–

**Figure 4.** Molecular structure of the L₂ ligand (thermal ellipsoids are shown at 30% probability).

has a similar topology as L₂ (Figure 4). This can be seen in the N4–N3–C2–N1 dihedral angle (68.9(2)°) compared with L₂ (–31.0(4)°), as well as the angles around C2 (N3–C2–O1 and N1–C2–O1, which are 118.0(2)° and 128.0(2)°, respectively. This can also be observed in the N4–N3, C2–O1 and N3–C2, N1–C2 bond lengths, which are 1.233(2), 1.217(2), and 1.462(3), 1.321(3) Å, indicating double and single bond character, respectively, as previously observed in ligand L₂. For details, see Table 2 and SI section.

**Figure 5.** Molecular structure of the L₃ ligand. Only one of the two independent molecules found in the asymmetric unit is shown (thermal ellipsoids are shown at 30% probability).

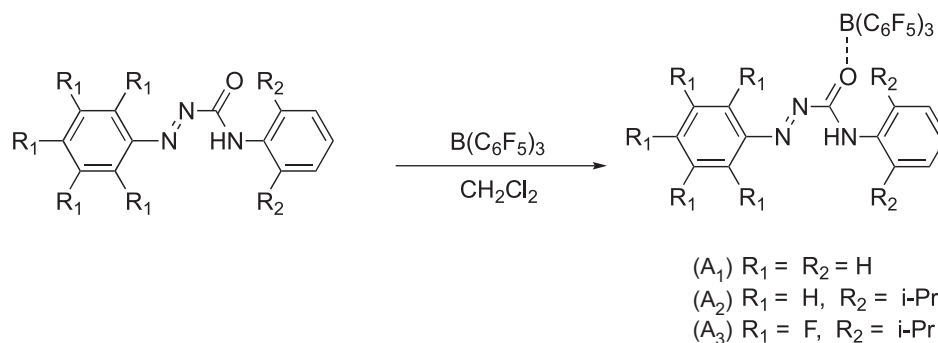
Reaction of the diazenecarboxamide ligand with B(C₆F₅)₃

We decided to investigate the diazenecarboxamide ligand's affinity for B(C₆F₅)₃ by stirring of the reaction mixture of the respective ligand (L₁–L₃) plus one equivalent of B(C₆F₅)₃ for 2 h at RT in dichloromethane (DCM), eventually yielding adduct A₁–A₃ [i.e., L₁–B(C₆F₅)₃] as a red crystalline solid in 100% isolated yield (Scheme 2). Single crystals of A₁–A₃ suitable for X-ray crystal structure analysis were obtained from DCM/pentane by the diffusion method.

The X-ray crystal structure analysis of compound A₁ (Figure 6), unlike the free ligand, features a U-shaped NNCN section of the framework (torsion angle N4–N3–C2–N1 is –16.8(3)°). The internal bonding situation is found to be asymmetric. The N3–N4 bond (1.249(2) Å) is markedly shorter than the opposite N3–C2 and N1–C2 bonds, 1.423(3) and 1.308(3) Å, and consequently the C2–O1 bond (1.260(3) Å) is shorter and consistent with a double bond character.

Carbon atom C2 is trigonal planar (sum of the bond angles at C2 360.0°). The B(C₆F₅)₃ Lewis acid is found to be coordinated with the oxygen atom (Figure 6). The boron atom shows a distorted tetrahedral coordination geometry with typical bond angles of 109.3(2)° (O1–B1–C31), 101.1(2)° (O1–B1–C41), and 108.8(2)° (O1–B1–C51). The C2–O1–B1 unit has a bent molecular geometry (angles C2–O1–B1 131.5(2)°). The O1–B1 bond length (1.565(3) Å) is within the typical O–B single bond range.^{38–40} The C2–O1 bond length is 0.043 Å longer than the distance in L₁ after coordination with BCF.

The IR spectrum of the A₁ borane adduct shows a strong C=O stretching band at $\tilde{\nu}$ = 1646 cm^{–1}, which is shifted by $\tilde{\nu}$ = 54 cm^{–1} to lower wavenumber compared to its parent L₁



Scheme 2. Synthetic pathway to the diazenecarboxamide-B(C₆F₅)₃ adduct.

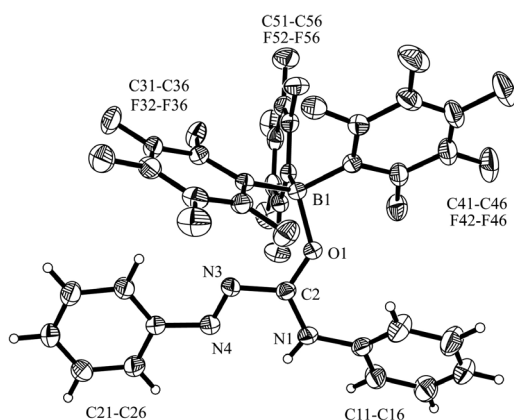


Figure 6. Molecular structure of the A₁ adduct (thermal ellipsoids are shown at 30% probability).

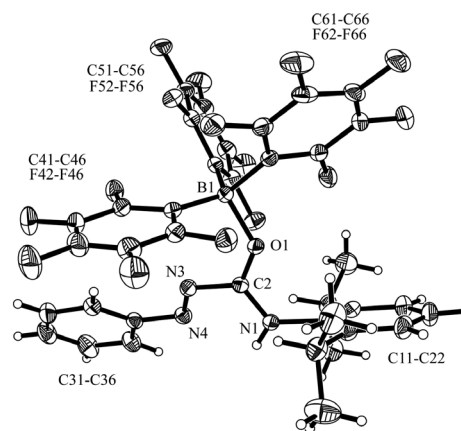


Figure 7. Molecular structure of the A₂ adduct (thermal ellipsoids are shown at 30% probability).

ligand. This is what would be expected from simple addition of a carbonyl to a strong Lewis acid: sharing of the oxygen lone pair with the boron atom effectively reduces overlap, making the double bond slightly weaker, consistent with what we found by the X-ray crystal analysis made above.

In the ¹H NMR spectrum of A₁, the N–H resonance at δ 9.22 ppm (in [D₂]-dichloromethane) is observed. The ¹¹B NMR spectrum features a typical four-coordinate boron resonance (δ –3.78 ppm), which is supported by a characteristically small Δδ (*p,m*) C₆F₅ chemical shift difference^{41–44} in the ¹⁹F NMR spectrum [δ –132.5 (*o*), –156.2 (*p*), –163.4 (*m*)]. Adduct A₁ shows a characteristic ¹³C resonance for the C=O–B units (δ ¹³C: 168.8 ppm).

Treatment of L₂ with one molar equivalent of B(C₆F₅)₃ in DCM at RT (2 h) led to complete conversion to A₂, which was isolated from the reaction mixture in quantitative yield. Single crystals of A₂ were obtained at RT from DCM/pentane by the diffusion method.

The X-ray crystal structure analysis of compound A₂ confirms the formation of a Lewis acid/Lewis base adduct, by coordination of BCF with the carbonyl functionality (Figure 7). As expected, the *U* configuration of the parent ligand L₂ is found to be nearly unperturbed upon adduct formation with B(C₆F₅)₃, as seen in A₁.

The boron atom has taken a distorted tetrahedral coordination geometry in the adduct. It features bond angles of 111.0(2)° (O1–B1–C41), 106.0(2)° (O1–B1–C51), and 102.1(2)° (O1–B1–C61). The O1–B1 bond length is 1.577(3) Å. The C2–O1 double bond (1.262(2) Å) is 0.043 Å longer than the C2–O1 bond in L₂ (a similar variation was observed in A₁). The central carbon atom C2 of the framework is trigonal planar (sum of the bond angles 359.8°). The central N=N double bond unit has a bond length of 1.252(2) Å, while the bond lengths of N3–C2 and C2–N1 are 1.432(3) and 1.309(3) Å, respectively. There is bond length alternation toward the carbonyl. An effect is also seen on the C2–N1 bond length, which is 0.024 Å smaller compared to that of the free ligand (Figure 4 and Table 2). Similarly to A₁, the IR spectrum of the borane adduct A₂ shows a strong C=O stretching band at $\tilde{\nu} = 1648 \text{ cm}^{-1}$, which is shifted by $\tilde{\nu} = 53 \text{ cm}^{-1}$ to lower wavenumbers compared to its parent ligand L₂, Table 1, consistent with the weakness of the carbonyl bond, which is seen from the X-ray crystal analysis mentioned above (Table 2).

In the NMR spectrum of A₂ the typical signals for the amide unit [¹H: δ 8.61 –NH; ¹³C: δ 164.2, (C=O–)] are observed. The ¹¹B NMR spectrum features a typical four-coordinate boron resonance (δ –4.41 ppm), and the

^{19}F NMR signals at δ -132.5 (*o*), -157.0 (*p*), and -164.0 (*m*) for the C_6F_5 substituents on boron.

Finally, the addition of one molar equivalent of $\text{B}(\text{C}_6\text{F}_5)_3$ to L_3 in DCM at RT (2 h) also led to complete conversion to A_3 , which was isolated from the reaction mixture in quantitative yield. Single crystals of A_3 were obtained in the same way as for A_1 and A_2 .

As expected, the crystal structure analysis (Figure 8) shows that the carbonyl functionality of L_3 is coordinated by $\text{B}(\text{C}_6\text{F}_5)_3$, (O1–B1 1.593(5) Å, angles O1–B1–C41 109.0(3)°, O1–B1–C51 105.5(3)°, O1–B1–C61 101.9(3)°). The bond length differences in the internal fragment's diazene double bond, N3–N4 1.242(4) Å, N3–C2 1.434(5) Å and N1–C2 1.306(5) Å, are in the range of those for the other adducts (A_1 and A_2).

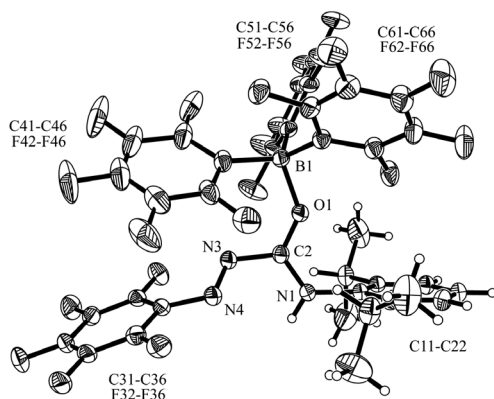


Figure 8. Molecular structure of the A_3 adduct. Only one of the two independent molecules found in the asymmetric unit is shown (thermal ellipsoids are shown at 30% probability).

In solution, compound A_3 has a ^{13}C NMR signal for the carbonyl carbon atom (C2) at δ 162.8 ppm. As expected, a single set of C_6F_5 resonances at δ -132.9 (*o*), -156.7 (*p*), and -163.1 ppm (*m*) was observed for the $\text{B}(\text{C}_6\text{F}_5)_3$ group coordinated with the carbonyl function (Scheme 2), and the corresponding ^{11}B NMR resonance was found at -6.02 . The C_6F_5 ring produced a single set of *o*-, *p*- and *m*- ^{19}F NMR resonances at δ -132.2 , -155.8 , and -162.3 ppm, respectively.

Conclusions

As stated in the introduction, our interest in this study was the synthesis and characterization of a variety of new ligands with additional functionality in the framework, which would allow the coordination to the metal center and to the other atoms. This means that there will be a free functional group, with lone electron pairs after the formation of the complexes. Scheme 1 provides a straightforward approach to generate diazenecarboxamide ligands in which

the steric bulk on the diazene and carboxamide nitrogens can be controlled by aromatic substituents. Furthermore, the diazenecarboxamide- $\text{B}(\text{C}_6\text{F}_5)_3$ adduct has been isolated and fully characterized. The binding of $\text{B}(\text{C}_6\text{F}_5)_3$ with the carbonyl functionality (Scheme 2) results in a unique adduct formation. This species has more acidic NH protons, as was shown by the shift of the resonance (more than 0.53 ppm) toward low field compared to the free ligand. This is due to a redistribution of electron density within the electronically delocalized ligand-BCF framework.

Supplementary Information

Supplementary data (further experimental and spectroscopic details, CCDC reference numbers 1005207-1005212 and potential energy profiles for the deprotonated form of ligands L_2 and L_3) are available free of charge at <http://jbcs.sbq.org.br> as PDF file.

Acknowledgements

The authors acknowledge the financial support by CONICYT through FONDECYT projects 1100286, 1130077 and Milenium Nucleus NC120082. M. E. acknowledges funding through a CONICYT PhD fellowship.

References

- Little, R. D.; Venegas, M. G.; *J. Org. Chem.* **1978**, *43*, 2921.
- Hashim, A. B.; Elie, A. J.; Noel, C.; *Tetrahedron Lett.* **1996**, *37*, 2951.
- Russ, H. W.; Tappe, H.; *Eur. Pat. Appl.* **1994**, 629, 667.
- Kurihara, S.; Yoneyama, D.; Nonaka, T.; *Chem. Mater.* **2001**, *13*, 2807.
- Ikeda, T.; Tsutumi, O.; *Science* **1995**, *268*, 1873.
- Sefkow, M.; Kattz, H.; *Tetrahedron Lett.* **1999**, *40*, 6561.
- Liu, Z. F.; Hashimoto, O. K.; Fujishima, A.; *Nature* **1990**, *347*, 658.
- Pieters, L.; Kosmrlj, J.; Lenarsic, R.; Kocevar, M.; Polanc, S.; *Arkivoc* **2001**, v, 42.
- Kosmrlj, J.; Kocevar, M.; Polanc, S.; *J. Chem. Soc., Perkin Trans. 1* **1998**, *23*, 3917.
- Song, D.; Ye, W.; Wang, Y.; Liu, J.; Li, Y.; *Organometallics* **2009**, *28*, 5697.
- Song, D.; Wu, J.; Ye, W.; Mu, H.; Li, Y.; *Organometallics* **2010**, *29*, 2306.
- Jenkins, J. C.; Brookhart, M.; *J. Am. Chem. Soc.* **2004**, *126*, 5827.
- Liu, J.; Li, Y.; Hu, N.; *J. Appl. Polym. Sci.* **2008**, *109*, 700.

14. Zai, S.; Gao, H.; Huang, Z.; Hu, H.; Wu, H.; Wu, Q.; *ACS Catal.* **2012**, *2*, 433.
15. Hu, H.; Zhang, L.; Gao, H.; Zhu, F.; Wu, Q.; *Chem. Eur. J.* **2014**, *20*, 3225.
16. Feng, Q.; Chena, D.; Feng, D.; Jiao, L.; Peng, Z.; Pei, L.; *Appl. Organomet. Chem.* **2014**, *28*, 32.
17. Wang, F.; Yuan, J.; Song, F.; Li, J.; Jia, Z.; Yuan, B.; *Appl. Organomet. Chem.* **2013**, *27*, 319.
18. Kolhatkar, N. A.; Monfette, A. M.; Lin, S.; Miri, M. J.; *J. Polym. Sci., Part A-1: Polym. Chem.* **2012**, *50*, 986.
19. Gates, D. P.; Svejda, S. K.; Onate, E.; Killian, C. M.; Johnson, L. K.; White, P. S.; Brookhart, M.; *Macromolecules* **2000**, *33*, 2320.
20. Wang, S.; Sun, W.; Redshaw, C.; *J. Organomet. Chem.* **2014**, *751*, 717.
21. Froese, R.; Musaev, D.; Morokuma, K.; *J. Am. Chem. Soc.* **1998**, *120*, 1581.
22. Liu, H.; Zhao, W.; Yu, J.; Yang, W.; Hao, X.; Redshaw, C.; Chen, L.; Sun, W.; *Catal. Sci. Technol.* **2012**, *2*, 415.
23. Boardman, B. M.; Valderrama, J. M.; Muñoz, F.; Wu, G.; Bazan, G. C.; Rojas, R.; *Organometallics* **2008**, *27*, 1671.
24. Shim, C. B.; Kim, Y. H.; Lee, B. Y.; Dong, Y.; Yun, H.; *Organometallics* **2003**, *22*, 4272.
25. Okada, M.; Nakayama, Y.; Ikeda, T.; Shiono, T.; *Macromol. Rapid Commun.* **2006**, *27*, 1418.
26. Azoulay, J. D.; Itiagaki, K.; Wu, G.; Bazan, G.; *Organometallics* **2008**, *27*, 2273.
27. Rojas, R.; Wasilke, J.; Wu, G.; Ziller, J. W.; Bazan, G.; *Organometallics* **2005**, *24*, 5644.
28. Rojas, R.; Galland, G.; Wu, G.; Bazan, G.; *Organometallics* **2007**, *26*, 5339.
29. Osichow, A.; Göttker-Schnetmann, I.; Mecking, S.; *Organometallics* **2013**, *32*, 5239.
30. Hooft, R. W. W.; COLLECT; Nonius B. V.: Delft, The Netherlands, 1998.
31. Otwinowski, Z.; Minor, W.; *Methods Enzymol.* **1997**, *276*, 307.
32. Otwinowski, Z.; Borek, D.; Majewski, W.; Minor, W.; *Acta Crystallogr.* **2003**, *A59*, 228.
33. Sheldrick, G. M.; *Acta Crystallogr.* **1990**, *A46*, 467.
34. Sheldrick, G. M.; *Acta Crystallogr.* **2008**, *A64*, 112.
35. Graphics XP, Bruker AXS Inc., Madison, Wisconsin, USA, 2000.
36. Wang, Y.; Wang, X.; Li, J. P.; Ian, D.; Wang, H.; *Synth. Commun.* **1997**, *27*, 1737.
37. Li, X.; Wang, Y.; Wang, J.; *J. Chem. Res-S* **2002**, (S), 284.
38. Xu, B.; Kehr, G.; Fröhlich, R.; Wibbeling, B.; Schirmer, B.; Grimme, S.; Erker, G.; *Angew. Chem., Int. Ed.* **2011**, *50*, 7183.
39. Kolychev, E. L.; Bannenberg, T.; Freytag, M.; Daniliuc, C. G.; Jones, P. G.; Tamm, M.; *Chem. Eur. J.* **2012**, *18*, 16938.
40. Neu, R. C.; Ouyang, E. Y.; Geier, S. J.; Zhao, X.; Ramos, A.; Stephan, D.; *Dalton Trans.* **2010**, *39*, 4285.
41. Birkmann, B.; Voss, T.; Geier, S. J.; Ullrich, M.; Kehr, G.; Erker, G.; Stephan, D. W.; *Organometallics* **2010**, *29*, 5310.
42. Dureen, M. A.; Stephan, D. W.; *J. Am. Chem. Soc.* **2010**, *132*, 13559.
43. Xu, B.; Alfonso, R.; Yanez, A.; Nakatsuka, H.; Kitamura, M.; Fröhlich, R.; Kehr, G.; Erker, G.; *Chem. - Asian J.* **2012**, *7*, 1347.
44. Voss, T.; Mahdi, T.; Otten, E.; Fröhlich, R.; Kehr, G.; Stephan, D. W.; Erker, G.; *Organometallics* **2012**, *31*, 2367.

Submitted: April 13, 2015

Published online: October 21, 2015